

**Part IV Bioelectronics**

**Section 1 Genetic Analysis**



## **Section 1 Genetic Analysis**

### **Chapter 1 Genosensor Technology Development**





# Chapter 1. Genosensor Technology Development

## Academic and Research Staff

Dr. Daniel J. Ehrlich, Dr. Mark A. Hollis, Dr. John Melngailis,<sup>1</sup> Dr. Dennis D. Rathman

## 1.1 Introduction

The primary objective of this cooperative work with the Houston Advanced Research Center (HARC) is to develop a novel method for automated, low-cost, high-throughput DNA sequence analysis. The overall goal is to demonstrate laboratory prototypes that provide a substantial increase in speed over the conventional DNA sequencing methods now used in biomedical, pharmaceutical, and agricultural industries.

The basic approach being taken is depicted in figure 1. In a hypothetical DNA sequencing test, a solution of single-stranded "target" DNA strands of identical but unknown sequence is washed onto a specialized microelectronic chip called a genosensor. The genosensor surface contains a large array of test sites, each site containing short pieces of single-stranded DNA known as "probes." These probes are chemically attached to the site. All probes in a given site are of like sequence, and the sequence for each site is unique on the chip. The target DNA strands will bond, or hybridize, very strongly to probes containing their exact Watson-Crick complement, but much less strongly to probes on other sites. The sites containing hybridized DNA are identified via electronic sensing on the chip, and this information is used by off-chip instrumentation to reconstruct the sequence of the target strands. MIT's role in this effort is primarily the design and fabrication of the genosensor chips.

## 1.2 Development of Genosensor Arrays for DNA Decoding

### Sponsor

Houston Advanced Research Center  
Contract HRC-HG00665-01

### Project Staff

Dr. Daniel J. Ehrlich, Dr. Dennis D. Rathman, Dr. Mark A. Hollis, Dr. John Melngailis

## 1.2.1 Genosensor Electronic-Detection Principle

The simplest electrical measurement that can be made at a test site to detect hybridization is probably a measurement of the change in local permittivity due to the addition of long target strands to the site. The complex permittivity  $\epsilon' - j\epsilon''$  of an aqueous solution containing DNA exhibits a dispersion around a relaxation frequency which is a function of the size and conformation of the DNA molecule. A measurement of the capacitance and/or conductance between two electrodes in the solution over a range of frequency can therefore differentiate between a site that contains only short probe strands and one that contains long target strands hybridized to the probe strands. From these measurements the relative permittivity  $\epsilon'$ , the dielectric loss  $\epsilon''$ , and the dissipation factor  $\epsilon''/\epsilon'$  can be obtained for the cell.

The ideal electrode structure in a test well consists of two parallel plates spaced so that the entire volume between them is filled by the hybridized DNA globules in aqueous solution. For the sizes of target DNA envisioned, this spacing ranges from approximately 200 to a few thousand angstroms. A practical, easily fabricated structure that approximates this ideal is an interdigitated design shown in figure 2. Fabricated by a combination of wet and dry etching with metal liftoff, this design can achieve the required spacings between the upper and lower electrodes at their edges.

## 1.2.2 Genosensor Fabrication Development

The primary emphasis of this grant is on the process development and feasibility exploration for the genosensor design of figure 2. For this chip, conventional 2- $\mu\text{m}$  photolithography, wet and dry etching techniques, and electron-beam evaporation and liftoff processes are used to fabricate an interdigitated electrode structure in which the opposing electrodes are separated vertically.

<sup>1</sup> Professor, Department of Electrical Engineering, University of Maryland, College Park, Maryland, as of September 1993.

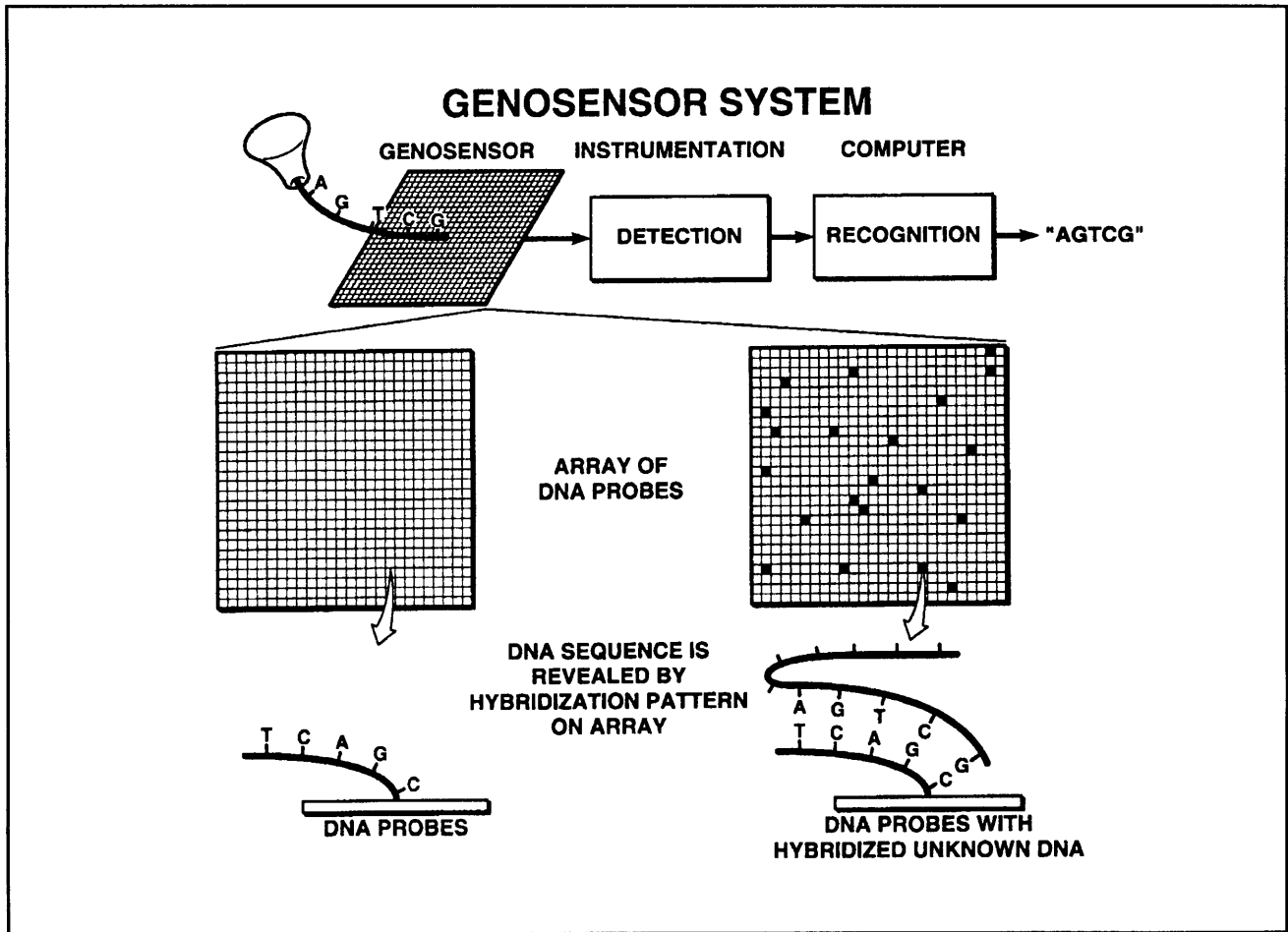


Figure 1. Conceptual genosensor system.

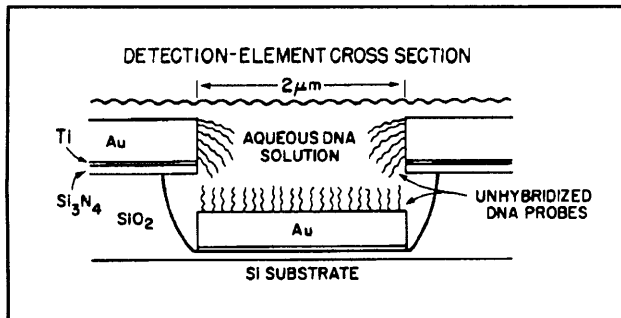
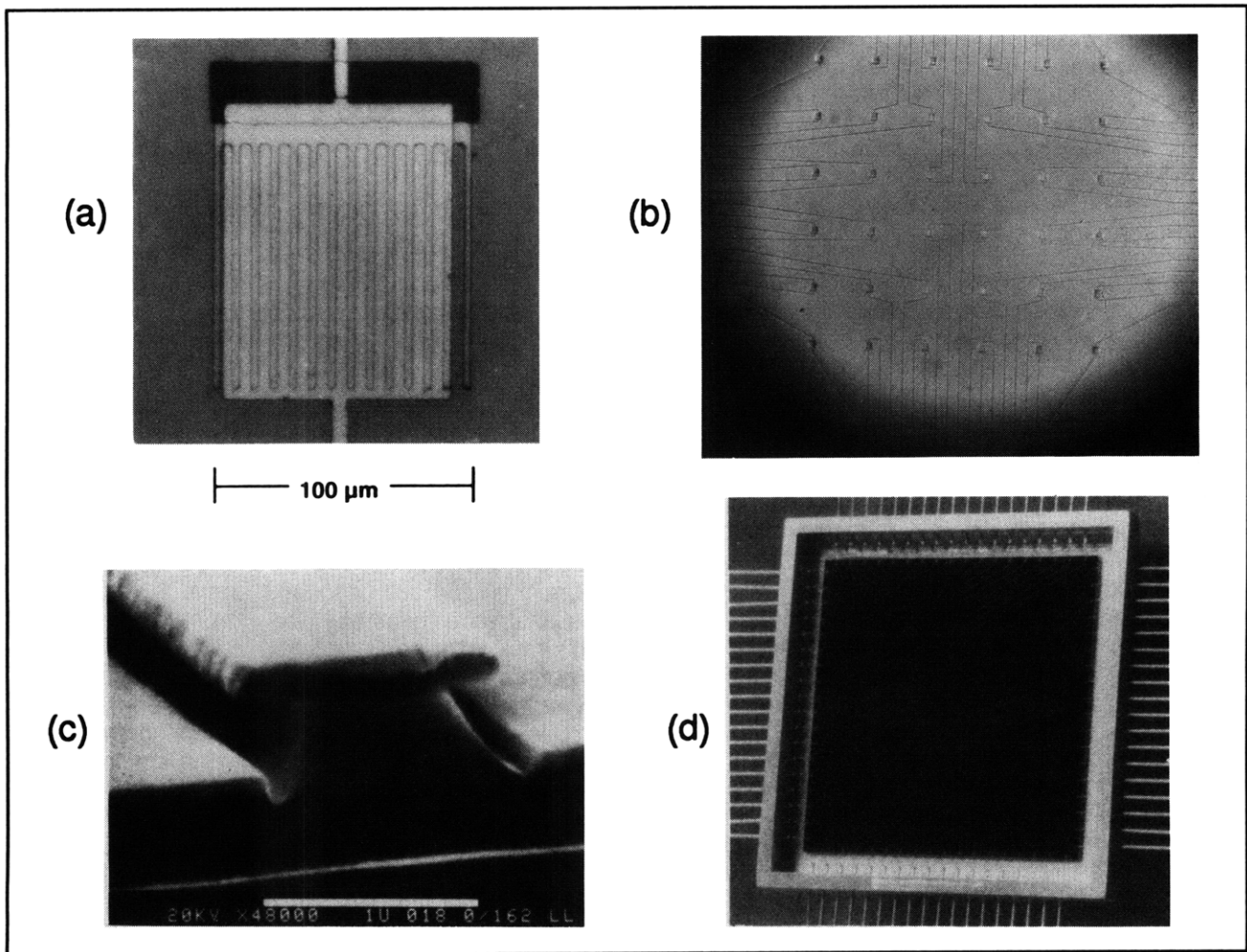


Figure 2. Electrode design for a permittivity genosensor. The unit cell shown is repeated many times across a test well to form an interdigitated test structure with the top Au electrodes connected to one access line and the bottom Au electrodes to the other.

During this past year, significant progress has been made in process development. A new 6x6 passive-array mask design has been completed and several genosensor chips have been fabricated, packaged, and delivered to HARC for testing. Figure 3 illustrates various aspects of the genosensor test chips. While the electrode-finger configuration was fixed at 2-μm width for both upper and lower electrodes, the

numbers of electrode fingers and the finger lengths were systematically varied from site to site on each chip. This was done primarily for a two-fold purpose: (1) to test relative signal sensitivity as a function of cell size, and (2) to aid in the evaluation of device yield. The largest single device is 800x800 μm, which is 64 times larger than our standard design. Since the primary fatal defect affecting device yield is a metal short between the opposing electrodes, a good yield for these large devices would likely project a very high yield for the standard devices. In addition, signal sensitivity should be greater for the large-area devices. Signal sensitivity can also be enhanced by bringing the opposing electrodes closer, either by using thicker evaporated metal films or by reducing the oxide etch depth. (This has been verified by some modeling work performed under contract HRC-HG00776-01; see section 3 below.) However, this increases the probability of shorts and thus lowers the yield. For electrode vertical gaps greater than 3000 Å, the device yield at the cell site is better than 90 percent. For gaps less than 2000 Å, the yield is less than 50 percent for the largest-area



**Figure 3.** Collection of photographs showing various views of a complete genosensor device. (a) Top view of the standard  $100\ \mu\text{m} \times 100\ \mu\text{m}$  single test cell. (b) Top view of the  $6 \times 6$  passive array of test cells. (c) Scanning electron micrograph (SEM) closeup of the interdigitated electrode fingers. (d) Genosensor chip in electronic package.

devices. Finally, the new design also eliminated one mask level and a difficult etching step.

The other significant development for the period was the implementation of Pt instead of Au as the electrode material. Pt offers several potential advantages as an electrode material compared to Au: (1) It is more compatible with Si fabrication technology than Au, (2) Pt seems to be preferred by the chemists for DNA probe attachment, and (3) Pt is more resistant to corrosion and electrolytic etching effects than Au in the rather hostile, conductive aqueous buffer solutions important to DNA chemistry.

There are some disadvantages to using Pt for electrode fabrication, however. Because there are no good resist-compatible etches, electron-beam evaporation and liftoff must be used for patterning of the cell electrodes rather than an etching process. We have found that Pt evaporations gen-

erate a fair amount of heat owing to the high melting temperature of Pt. This adversely affects the photoresist which makes liftoffs difficult and necessitates additional cleaning procedures to ensure reliability of DNA attachment chemistry. Recent device wafers using reduced Pt-evaporation rates and additional resist postbaking have resulted in much improved device yield and surface cleanliness. Pt also has problems related to stress which limit the metal thickness that can be used and Pt is more resistive than Au (which may affect signal sensitivity—this topic is still under investigation but is probably not a problem).

An additional problem that we have encountered is breakage in the Pt interconnect lines that connect the bonding pads at the periphery of the chip to the biosites clustered in the center. Initially, we believed that this problem was in part due to the rather long and narrow ( $3\text{-}\mu\text{m}$  wide) nature of these lines. Further investigation and mapping of several

device wafers show that the breakages seem to be clustered in consistent regions from wafer to wafer, yet there appear to be no obvious problems on the photolithographic masks. This is still being investigated. In the meantime, we are using our direct-write laser metal-deposition capability to repair the broken lines with very good success. Pt is our preferred laser-write material, another advantage for using Pt for genosensors.

Over this time period, we have delivered 14 packaged device chips to HARC for this project. At present, several more wafers are in various stages of processing.

### 1.2.3 Genosensor Test Results

The results of electrical tests on a genosensor test cell are illustrated in figure 4. In this experiment, 12mer DNA probes (12 nitrogenous bases in a single strand) were attached to the Pt electrodes of a test well. Permittivity measurements were recorded using an impedance bridge connected to the leads of the test site via the genosensor package shown in figure 3. Next, high molecular weight (4000 base pairs) target DNA was puddled on the electrodes and the measurements repeated after approximately 50 minutes. Complementary target and probe DNA strands were used in this experiment to insure that hybridization occurred. From the measurements, the dissipation factor as a function of frequency was extracted for both the nonhybridized-probe case and the hybridized case (probe plus target). The nonhybridized probes exhibited maximum energy absorption at 800 kHz, while the hybridized DNA displayed maximum absorption at 80 kHz, a factor of 10 in frequency discrimination. Further, the nonhybridized probes exhibited a dissipation factor of 20 at the peak, while the corresponding value for the hybridized case was 4. These results, though preliminary, are very encouraging as they indicate that sufficient discrimination between hybridized and nonhybridized DNA can be achieved. For further discussion see section 3 below.

## 1.3 Microdetection Technology for Automated DNA Sequencing

### Sponsor

Houston Advanced Research Center  
Contract HRC-HG00776-01

### Project Staff

Dr. Daniel J. Ehrlich, Dr. Dennis D. Rathman, Dr. Mark A. Hollis, Dr. John Melngailis

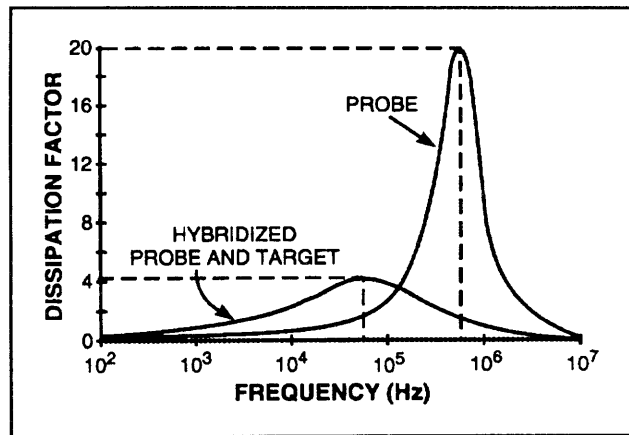


**Figure 4.** Measured dissipation factor data from a test site containing hybridized probe and target DNA plotted for comparison with data from a site containing nonhybridized-probe DNA.

The primary emphasis of this effort is to complement the program described above by optimizing the electrode geometry for maximum sensitivity. This task is being undertaken using a two-pronged experimental and theoretical approach. In the experimental approach, the electrode-finger geometry is systematically varied by varying the finger linewidth or by placing the opposing electrodes on the same horizontal plane (see figure 5 and compare to figure 2). This is in contrast to the cell-geometry variations with a fixed electrode finger width of  $2\ \mu\text{m}$  described in the previous section. Assuming that the DNA attachment chemistry is not significantly affected by these electrode variations, measurements of dissipation factor, loss, relative permittivity, and the relaxation frequency should yield direct information on relative sensitivity. During the past year we have supplied 12 packaged chips to HARC of this type for testing. Many of these chips are currently being tested. In the theoretical approach, computer modeling is used to determine the relative sensitivities of electrode geometries using known or measured properties of the attached DNA layers. The combination of the electrical measurements and computer modeling should allow us to optimize the electrode geometry and also provide the insight necessary to develop a physical model for the dispersion effects exhibited by DNA in aqueous solutions.

During this past year an electromagnetic-simulation package was purchased from ANSOFT that solves Maxwell's equations in two dimensions. Recently, this software has been upgraded to handle materials with complex permittivities such as DNA. Figure 6 shows the electrode geometry in cross section and some equipotential contours from a solution generated by ANSOFT with the metal fingers



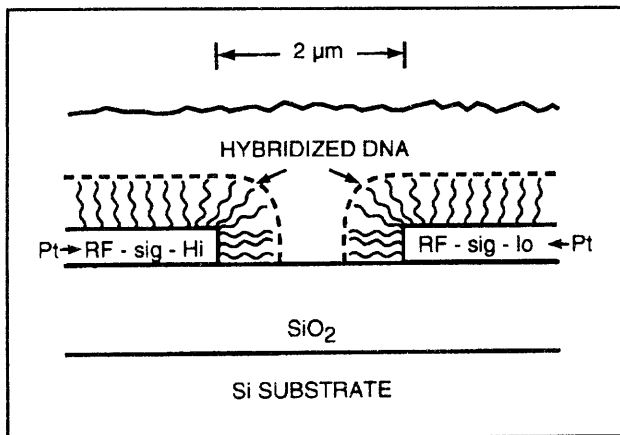


**Figure 5.** Permittivity-genosensor electrode design in which the opposing electrodes are on the same horizontal plane. The data of figure 4 was acquired using this electrode design.

appropriately biased. Note the hybridized DNA layer attached to the metal electrodes. The input parameters for the model are the cell geometry, applied bias, the real and imaginary parts of the permittivities for all of the materials, and the signal frequency. The simulation yields the complex admittance at the electrodes modeled as a parallel resistance,  $R_p$ , and capacitance,  $C_p$ , for the genosensor cell. These values can in turn be used to calculate  $\epsilon'$ ,  $\epsilon''$ , and the dissipation factor from the following relations:

$$C_p = \epsilon' C_o$$

$$\epsilon'' = 1/\omega R_p C_o$$

$$\epsilon''/\epsilon' = 1/\omega R_p C_p$$

where  $C_o$  is the capacitance between the electrodes in vacuum. The parallel  $R_p$  and  $C_p$  obtained in this way yield a simplified equivalent circuit for the genosensor cell, which in turn can be used to simulate the behavior of the cell in a circuit environment that may include switching transistors.

The most immediate use for the modeling results, however, is to infer the dispersion characteristics for the DNA in solution by comparing the calculations with the experimental results. The experimental data shown in figure 4 were obtained for the probe and hybridized DNA using the electrode geometry of figure 5, as described in the previous section. Assuming a 4000-Å-thick DNA layer for the hybridized case, a dissipation factor of 4 (in agreement with the experimentally obtained value at a signal frequency of 80 kHz) can be obtained with a peak

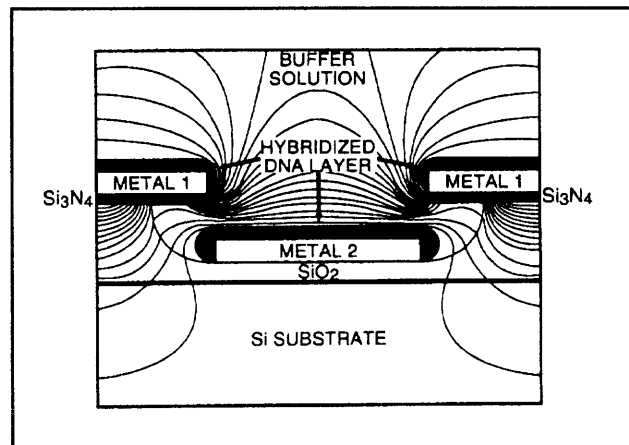


**Figure 6.** Cross section of genosensor electrode geometry and contours of constant electric potential with the electrodes biased for test.

value of  $\epsilon''$  of 900 for this geometry. This value of  $\epsilon''$  is very consistent with literature values for similar DNA. However, for the nonhybridized case, where a dissipation factor of 20 was measured, the experimental data cannot be fit by any simple adjustment of DNA permittivity or loss in the model. Such a large loss mechanism for the nonhybridized-probe case might be explainable by a preferential and ordered alignment of the short negatively-charged DNA probes on the electrode surfaces. These probes may act as a regular array of high-Q mechanical oscillators efficiently absorbing energy from the alternating electric field at a characteristic resonant frequency. An alternative explanation might be related to the electric dipole formed by the negatively charged DNA probes and the positive ions in solution. This dipole layer, as it resonates with the applied AC field, could in turn modulate the conductivity of the buffer solution in the vicinity of the electrodes, giving rise to the characteristic peak. In any case, this phenomenon is currently under intense investigation.

#### 1.4 Publications

Beattie, K.L., M.D. Eggers, J. Shumaker, M.E. Hogan, R. Varma, J.L. Lamture, M.A. Hollis, D.J. Ehrlich, and D.D. Rathman. "Genosensor Technology," *Clin. Chem.* 39(4): 719-722 (1993).

Rathman, D.D., M.A. Hollis, J. Melngailis, D.J. Ehrlich, M.E. Hogan, T. Powdrill, J.L. Lamture, M.D. Eggers, K.L. Beattie, R. Varma, and R. Gangadharan. "Electronic Permittivity Detection for DNA Sequencing by Hybridization." Paper presented at the 1993 International Workshop on DNA Sequencing by Hybridization, The Woodlands, Texas, October 29-30, 1993.

